Electronic supplementary Information

Superhydrophilic and underwater superoleophobic nanofibrous membrane with hierarchical structured skin for effective oil-in-water emulsion separation

Jianlong Ge,[a,b] Jichao Zhang,[a,b] Fei Wang,[a,b] Zhaoling Li,[a,b] Jianyong Yu,[b] and Bin Ding*[a,b]

[a] Key Laboratory of Textile Science & Technology, Ministry of Education, College of Textiles, Donghua University, Shanghai 201620, China.
[b] Nanofibers Research Centre, Modern Textile Institute, Donghua University, Shanghai 20051, China
Email: binding@dhu.edu.cn

Materials: Polyacrylonitrile (PAN, Mw = 90,000) was purchased from Kaneka Co., Ltd., Japan. SiO_2 nanoparticles (diameter of particles, 7-40 nm), sodium dodecyl sulphate (SDS), oil red (sudan III), methylene blue (MB) were purchased from Aladdin Chemistry Co. Ltd, China. Dimethylfomamide (DMF), n-hexane, petroleum ether, dichloroethane, and hexadecane were obtained from Shanghai Chemical Reagents Co., Ltd., China. Diesel oil was provided by the China National Petroleum Corporation. Pure water was obtained via using a Heal-Force system. All chemicals were of analytical grade and were used as received without further purification.

Fabrication of the PAN nanofibrous membranes: Firstly, precursor solution was prepared by dissolving the sufficiently dried PAN powder in DMF at a concentration of 12 wt%. Then, a DXES-3 electrospinning machine (SOF Nanotechnology Co., China) was used to perform the electrospinning, meanwhile, the solution was loaded into a group of syringes (5 of side by side) capped with 6-G metal with a constant feed rate of 1.5 ml per hour. The syringes could scanning horizontally with a range of 50 cm. The working voltage applied to the needle tips was fixed to 25 kV to ensure the stability of the generated jet streams and sufficient electric field intensity. The resultant nanofibers were collected by a nonwoven fabrics coated grounded metallic rotating roller with a rotation rate of 50 rpm. The distance from needle tips to the surface of roller was 20 cm. The temperature and relative humidity during the

electrospinning were fixed at 25 ± 2℃ and 45 ± 5℃, respectively. The electrospinning process was continuously conducted for 4 hours.

Construction of the hierarchical structured microspheres skin: Firstly, to find out an optimized PAN concentration for the conctruction of microspheres layer, pure dilute PAN solutions with different concentrations of 1, 2, 3, and 4 wt% were prepared. The electrospraying was performed by loading the precursor solutions onto the same machine of electrospinning (DXES-3 electrospinning machine), the feed rate of the solution were fixed at 1.0 ml per hour. A voltage of 25 kV was applied onto the needle tips to conduct the atomization of the precursor solutions. The generated microspheres were directly deposited on the surface of the as-prepared nanofibrous membranes coated on a grounded metallic rotating roller with a rotation rate of 50 rpm. The distance from needle tips to the surface of nanofibrous membranes was fixed at 20 cm. During the whole electrospraying process, the temperature and relative humidity were fixed at 25 ± 2℃ and 55 ± 5℃, respectively. Each electrospraying process was performed for 4 hours without breaking. Subsequently, SiO_2 NPs were dispersed in DMF at the concentration of 1, 2, 4, and 6 wt%, respectively, under the treatment of ultrasonic for 30 min. Then a certain amount of PAN powder was dissolved in the corresponding SiO_2 NPs/DMF suspensions at a fixed concentration. The composite membranes with SiO_2 NPs in the microspheres at the concentration of 1, 2, 4, and 6 wt% was noted as SiO_2/NFM-1, SiO_2/NFM-2, SiO_2/NFM-4, SiO_2/NFM-6, respectively.

Preparation of the emulsions: For oils (taken n-hexane, petroleum ether as examples) with low viscosity, surfactant-free oil-in-water emulsions were prepared by mixing different oils and water in a volume ratio of 1:9 and sonicating the mixture for 1 h to get an emulsified, milky solution. To prepare the surfactant-stabilized oil-in-water emulsion, sodium dodecyl sulfonate (0.1 mg/mL) was used as the emulsifier, and the volume ratio of oils and water was fixed to 1:99, then the mixture was sonicated for 0.5 h to produce white emulsions. For oils

(taken hexadecane, diesel oil as examples) with higher viscosity, surfactant-free oil-in-water emulsions were prepared by mixing oils and water in a volume ratio of 1:9 and the mixtures were for 1 h to get an emulsified, milky solution. The as-prepared surfactant-free oil-in-water emulsion could keep stable for 4 h without obvious demulsification. To prepare the surfactant-stabilized oil-in-water emulsion, sodium dodecyl sulfonate (0.1 mg/mL) was used as the emulsifier, and the volume ratio of oils and water was fixed to 1:99, then the mixture was sonicated for 0.5 h to produce white emulsions. The as-prepared surfactant-stablized oil-in-water emulsion could keep stable for more than 12 h without obvious demulsification.

Oil/water separation experiments: The oil-in-water emulsion separation performance of the membranes were evaluated based on the dead-end filtration method. The membranes were fixed between two vertical glass tubes with the inner diameter of 16 mm. Upon conducting the emulsion separation the membranes were pre-wetted at first, then the as-prepared emulsions were feed directly onto the membrane with the water spontaneously permeated. A peristaltic pump was employed to continuously feed the solutions to keep a relatively stable liquid level (10 ± 0.5 cm). The whole separation process was driven under the gravity of solutions. The fluxes for different membranes were determined by calculating the volume of water permeated within 1 min.

Characterizations: The morphologies of the membranes were characterized using a scanning electron microscopy (Tescan Vega 3). A field emission transmission electron microscopy (FE-TEM, JEM-2100F, JEOL Ltd., Japan) was employed study the dispersion of nanoparticles inside the polymer matrix. The N_2 adsorption-desorption isotherms were recorded via a physisorption analyzer (Micromeritics ASAP 2020). Water contact angle (WCA), oil contact angle (OCA), and oil sliding angle (OSA) were tested by using a contact angle goniometer (Kino SL200B). The underwater oil contact angle hysteresis (OCAH) was measured based on the increment and decrement method. The underwater oil adhesion forces were measured by employing a high-sensitivity micro-electro-mechanical balance system

(Data-Physics DCAT11), 1,2-dichloroethane was used as the detected oil. The porous structures were analyzed using a capillary flow porometer (Porous Materials Inc CFP-1100AI). The tensile mechanical properties of the membranes were studied using a tensile tester (XQ-1C). The size distribution of the oil droplets in the oil-in-water emulsions were characterized by the optical microscopy (Olympus VHS3000). The oil content in the filtrate was measured using a total organic carbon analyzer (Shimadzu TOC-L).

Calculation method of the adhesion work: The adhesion works of the oil and water on the surface of the relevant membrane were calculated by the Young Dupré's Equation: $W_{ad} = \gamma_{lg}(1 + \cos\theta_{lv})$, where the Wad is the adhesion work, the γ_{lv} is the surface tension of liquid/air interface, and the θ_{lv} is the relevant liquid contact angle in air. For the pristine NFM, both the WCA and OCA are 0° in air. And the surface tension in air for water and dichloromethane are 72 mN m^{-1} and 23 mN m^{-1}, respectively. Consequently, for water, the $W_{ad} = 72 \times (1 + \cos0°) = 144$ mN m^{-1}. For dichloromethane, the $W_{ad} = 23 \times (1 + \cos 0°) = 46$ mN m^{-1}.

Estimation of the liquid adhesion forces: In addition, the corresponding water retention force was also estimated based on the WCAH and the droplet volume (10 μL) using the followed equations:

$$F_r = (2/\pi)\gamma_{ow}D_c(\cos\theta_R - \cos\theta_A) \quad \text{(Equation S1)}$$

$$D_c = 2(6V/\pi)^{1/3}\{\tan(\theta_A/2)[3+\tan^2(\theta_A/2)]\}^{-1/3} \quad \text{(Equation S2)}$$

Where F_r is the retention force, γ_{ow} is the interface tension of oil and water, D_c is the contact diameter, θ_A is the advancing contact angle, θ_R is the receding contact angle, V is the volume of the droplet.

The determination of intrusion pressure: According the wetting models shown in Figure 4b, the intrusion pressure (Δp) were estimated based on the Laplace theory:

$$\Delta p = 2\gamma/r = -2\gamma\cos\theta_a/R \quad \text{(Equation S3)}$$

where Δp is the intrusion pressure, γ is the surface tension, r is the radius of curvature, θ_a is the advancing contact angle of the liquid on the surface of membrane and fibers, R is the

radius of the pores. During the oil/water seapration, on the top surface of the membrane, γ is the interface tension between oil and water. Meanwhile, the θ_a of oil was > 90° due to its underwater superoleophobiicty. As a consequence, the Δp of oil on the top surface of the membrane is > 0. Therefore, the oil phase could not penetrate into the membrane due to the pressure sustained by the hierarchical structured skin. Whereas, the Δp for water is < 0 condidering the superhydrophilicity of the membrane in air, where the θ_a of water is ~0°, resulting a capillary effect for the transport of water.

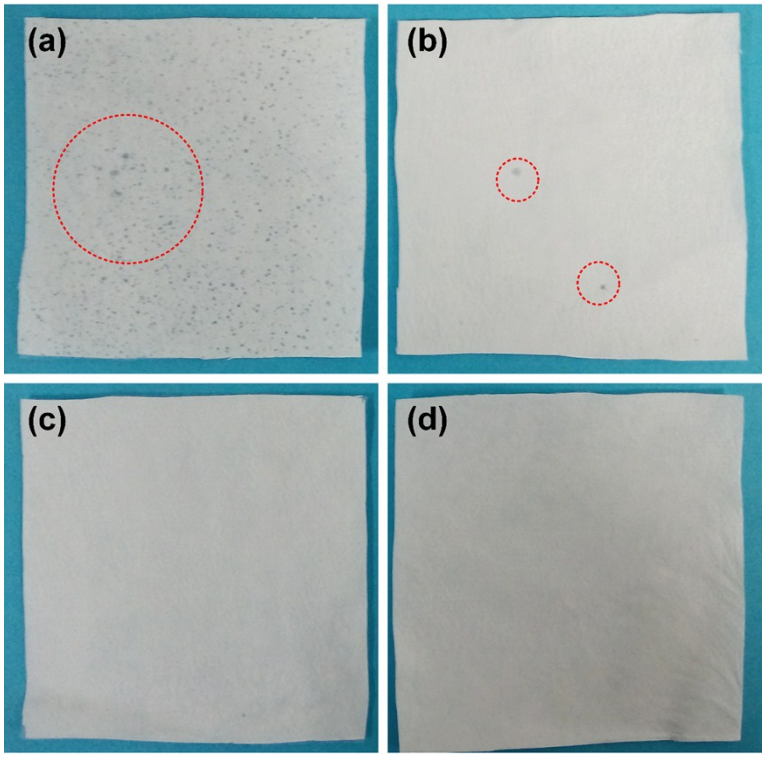

Fig. S1 Digital photographs of the composite membranes derived from dilute solutions with different PAN concentration: (a) 1, (b) 2, (c) 3, and (d) 4 wt%.

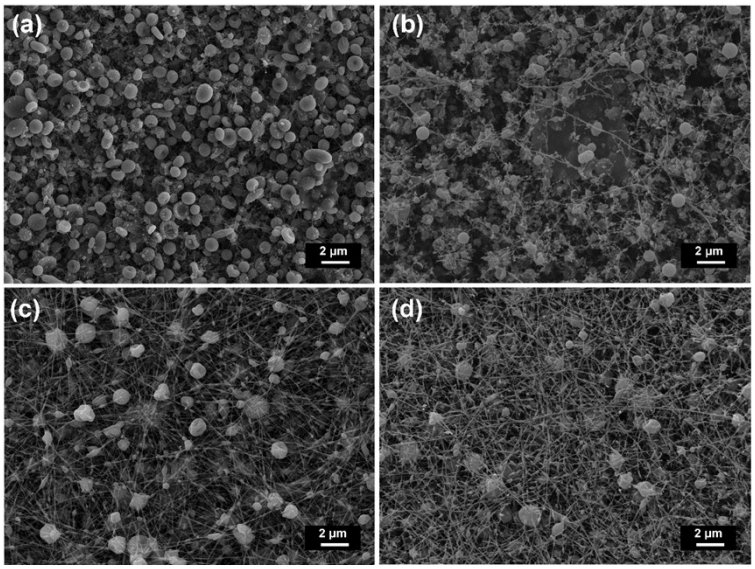

Fig. S2 SEM images of the composite membranes derived from dilute solutions with different PAN concentration: (a) 1, (b) 2, (c) 3, and (d) 4 wt%.

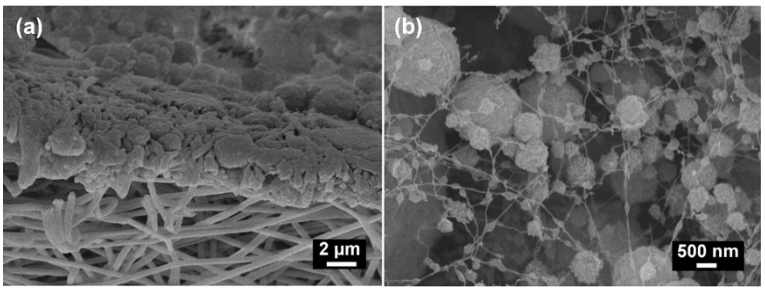

Fig. S3 Cross sectional SEM images (a), and high magnified top viewed SEM images of the SiO_2 /NFM-4.

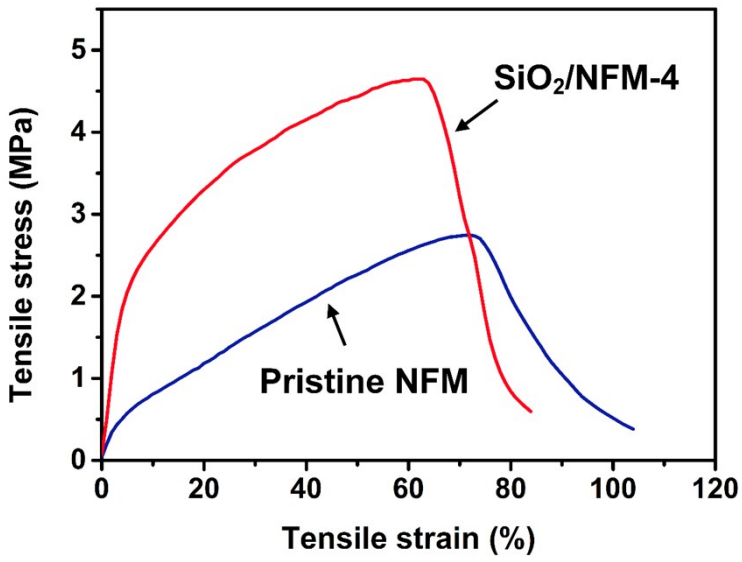

Fig. S4 Tensile stress-strain curves of pristine NFM and the relevant composite membranes.

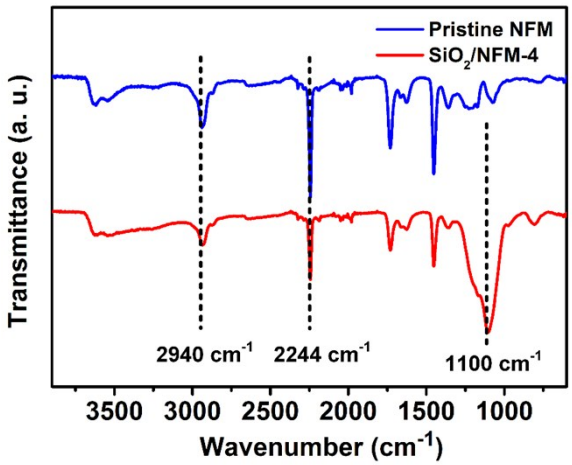

Fig. S5 FT-IR spectra of the pristine NFM and the relevant composite membranes.

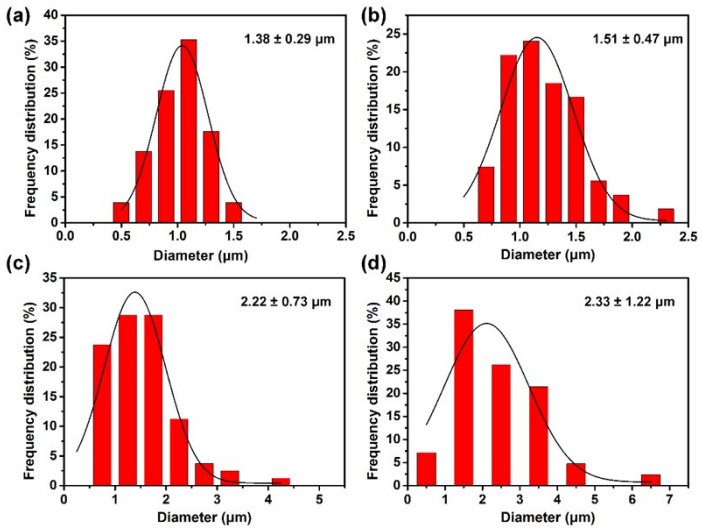

Fig. S6 Diameter distribution of the microspheres on the surface of the corresponding membranes: (a) SiO_2/NFM-1, (b) SiO_2/NFM-2, (c) SiO_2/NFM-4, (c) SiO_2/NFM-6.

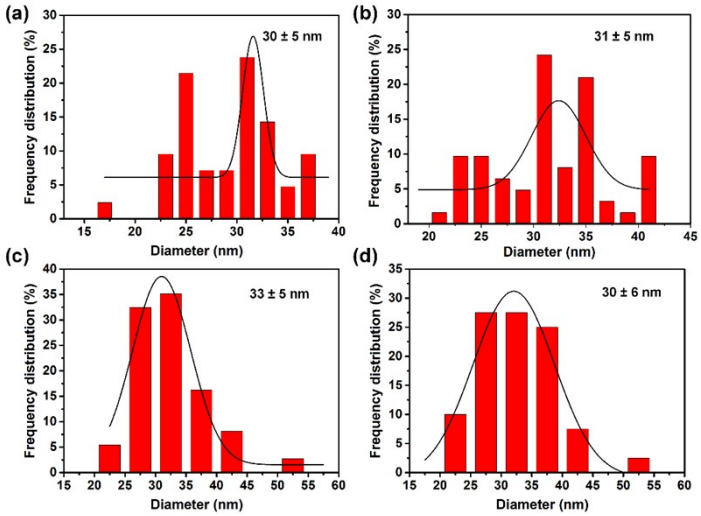

Fig. S7 Diameter distribution of the filaments connecting with the microspheres on the surface of the corresponding membranes: (a) SiO_2 /NFM-1, (b) SiO_2 /NFM-2, (c) SiO_2 /NFM-4, (c) SiO_2 /NFM-6.

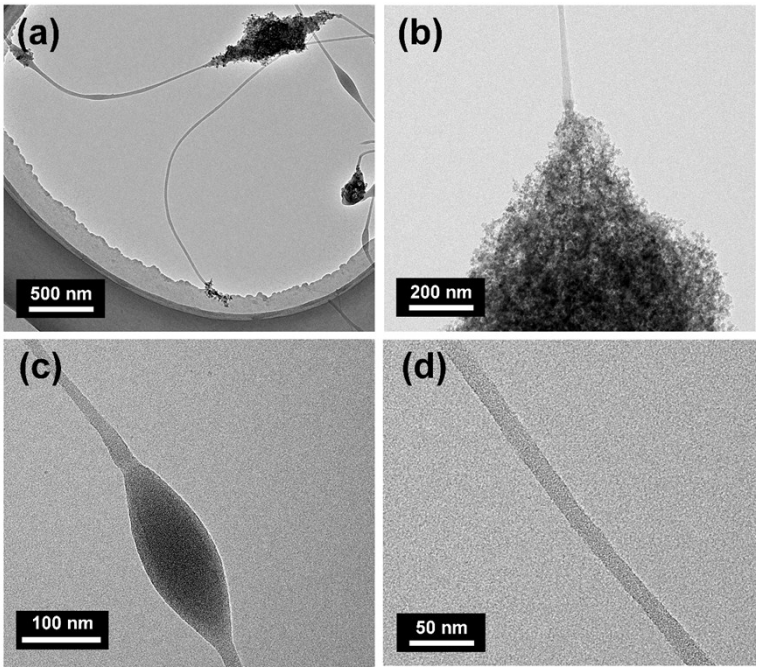

Fig. S8 TEM images of the microspheres (a and b), and the filaments (c and d) on the surface of SiO_2 /NFM-6.

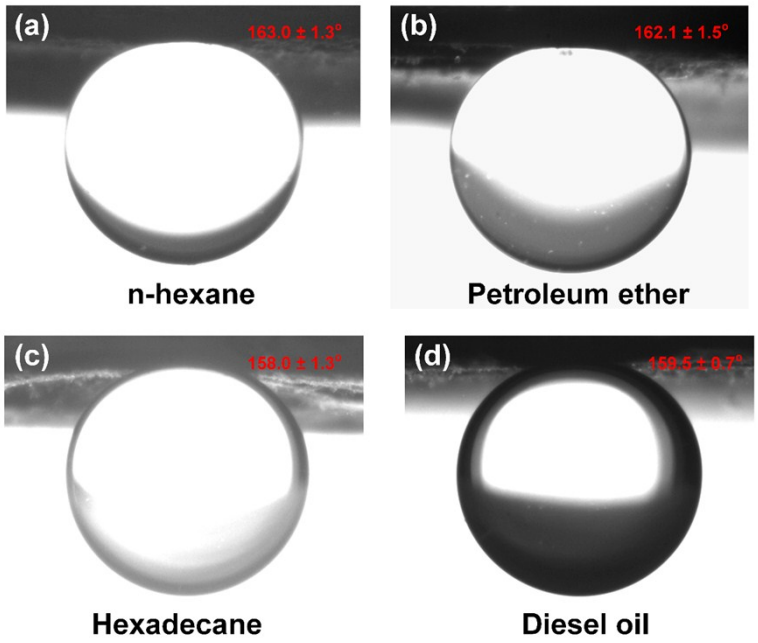

Fig. S9 Under water OCAs of different oils on the surface of SiO_2 /NFM-4.

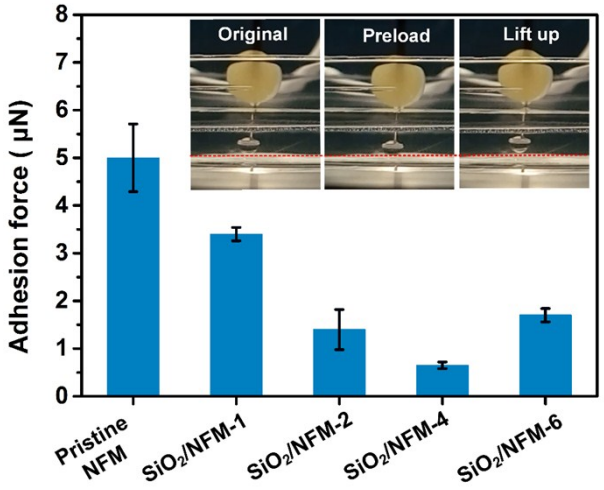

Fig. S10 Measured under water oil adhesion forces of oil on the surface of different membranes.

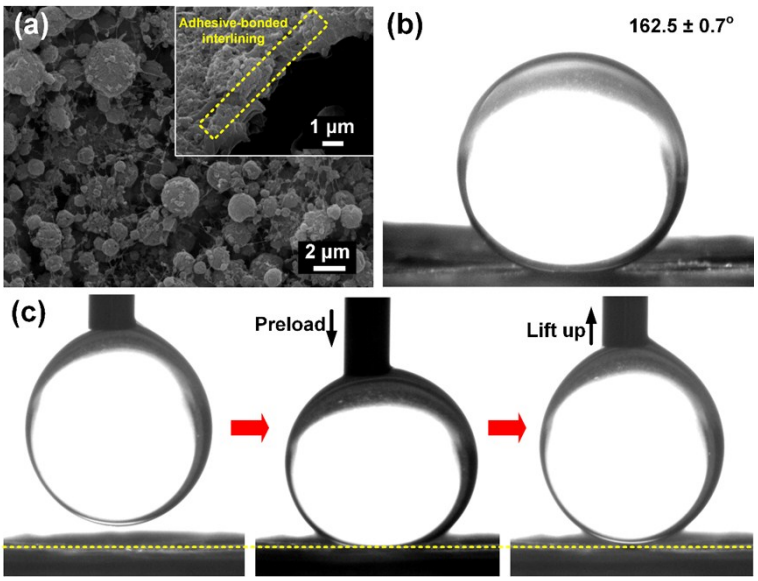

Fig. S11 (a) SEM images, (b) underwater OCA, and (c) dynamic oil repel property of SiO_2 /NFM-4 after after ultrasonic treatment for 5 h.

Table S1 Permeation fluxes of the SiO_2/NFM-4 for separating the oil-in-water emulsions in comparison with the separation membranes in literatures.

Sample	Pressure	Surfactant-free emulsions	Surfactant-stabilized emulsions	Literature
PDA/PEPA coated membrane	0.1 bar	34096 L m^{-2} h^{-1} bar^{-1} (hexane/water)	10000 L m^{-2} h^{-1} bar^{-1} (Teen 20/hexane/water)	Ref S1
TiO_2/CNT network film	0.05 bar	26410 L m^{-2} h^{-1} bar^{-1} (petroleum ether/water)	15690 L m^{-2} h^{-1} bar^{-1} (SDS/hexadecane/water)	Ref S2
TiO_2/PVDF membrane	0.9 bar	-	605 L m^{-2} h^{-1} (SDS/hexadecane/water)	Ref S3
PETMPEG/PVDF membrane	0.2 bar	-	800 L m^{-2} h^{-1} bar^{-1} (SDS/hexadecane/water)	Ref S4
PAA-g-PVDF membrane	0.1 bar	2320 L m^{-2} h^{-1} (hexadecane/water)	1140 L m^{-2} h^{-1} (SDS/hexadecane/water)	Ref S5
SiO_2/NMF-4	**Gravity (~0.01 bar)**	**6290 L m^{-2} h^{-1} (hexane/water)**	**1120 L m^{-2} h^{-1} (SDS/hexane/water)**	**This work**

Supplementary Discussion

Optimization of the concentration of dilute PAN solution

Fig. S1 depicts the digital photographs of the composite membranes derived from dilute solutions with different PAN concentration. It can be found that there were obvious defects on the surface of the membranes when the concentration of PAN < 3 wt%, which was attributed to the excess solvent remained in the electrospraying droplets. Meanwhile, when we further increase the PAN concentration the defects disappeared and the morphology of the obtained materials changed from microspheres to fibers at a higher PAN concentration (Fig. S2), this phenomenon was attributed to the increased viscosity of the solution, which could effectively prevent the jet from collapsing into droplets before the solidification.[S6,S7] For the sake of constructing a uniform skin layer consisting both nanofilaments and microspheres, we choose 3 wt% PAN for the further experiments.

Reference

S1 Y. Z. Cao, N. Liu, W. F. Zhang, L. Feng, Y. Wei, *ACS Appl. Mater. Interfaces* 2016, **8**, 3333.

S2 S. J. Gao, Z. Shi, W. B. Zhang, F. Zhang, J. Lin, *ACS Nano* 2014, **8**, 6344.

S3 H. Shi, Y. He, Y. Pan, H. H. Di, G. Y. Zeng, L. Zhang, C. L. Zhang, *J. Membr. Sci.* 2016, **506**, 60.

S4 T. Yuan, J. Q. Meng, T. Y. Hao, Z. H. Wang, Y. F. Zhang, *ACS Appl. Mater. Interfaces* 2015, **7**, 14896.

S5 W. B. Zhang, Y. Z. Zhu, X. Liu, D. Wang, J. Y. Li, L. Jiang, J. Jin, *Angew. Chem.-Int. Edit.* 2014, **53**, 856.

S6 H. Fong, I. Chun, D. Reneker, *Polymer* 1999, **40**, 4585.

S7 Y. J. Yang, S. C. Zhang, X. L. Zhao, J. J. Yu and B. Ding, *Sep. Purif. Technol.* 2015, **152**, 14.